Side Chains Control Dynamics and Self-Sorting in Fluorescent Organic Nanoparticles

ARTICLE *in* ACS NANO · DECEMBER 2012

Impact Factor: 12.88 · DOI: 10.1021/nn305477u · Source: PubMed

Side Chains Control Dynamics and Self-Sorting in Fluorescent Organic Nanoparticles

Adrien Kaeser,[†] Irén Fischer,[†] Robert Abbel,[‡] Pol Besenius,[‡] Debarshi Dasgupta,[†] Martijn A. J. Gillisen,[‡] Giuseppe Portale,[§] Amy L. Stevens,[⊥] Laura M. Herz,[⊥] and Albertus P. H. J. Schenning[†,*]

[†]Laboratory of Functional Organic Materials and Devices and [‡]Laboratory of Macromolecular and Organic Chemistry, Eindhoven University of Technology, P.O. Box 513, 5600 MB Eindhoven, The Netherlands, [§]Netherlands Organization for Scientific Research (NWO), European Synchrotron Radiation Facility (ESRF), DUBBLE-CRG, Grenoble, F-38043, France, and [⊥]Clarendon Laboratory, Department of Physics, University of Oxford, Parks Road, Oxford, OX1 3PU, United Kingdom

ABSTRACT To develop fluorescent organic nanoparticles with tailored properties for imaging and sensing, full control over the size, fluorescence, stability, dynamics, and supramolecular organization of these particles is crucial. We have designed, synthesized, and fully characterized 12 nonionic fluorene co-oligomers that formed self-assembled fluorescent nanoparticles in water. In these series of molecules, the ratio of hydrophilic ethylene glycol and hydrophobic alkyl side chains was systematically altered to investigate its role on the above-mentioned properties. The nanoparticles consisting of π-conjugated oligomers containing polar ethylene glycol side chains were less stable and larger in size, while nanoparticles self-assembled from oligomers containing nonpolar pendant chains were more stable, smaller, and generally had a higher fluorescence quantum yield. Furthermore, the dynamics of the molecules between the nanoparticles was enhanced if the number of hydrophilic side chains increased. Energy transfer studies between naphthalene and benzothiadiazole fluorene co-oligomers with the same side chains showed no exchange of molecules between the particles for the apolar molecules. For the more polar systems, the exchange of molecules between nanoparticles took place at room temperature or after annealing. Self-assembled nanoparticles consisting of π-conjugated oligomers having different side chains caused self-sorting, resulting either in the formation of domains within particles or the formation of separate nanoparticles. Our results show that we can control the stability, fluorescence, dynamics, and self-sorting properties of the nanoparticles by simply changing the nature of the side chains of the π-conjugated oligomers. These findings are not only important for the field of self-assembled nanoparticles but also for the construction of well-defined multicomponent supramolecular materials in general.

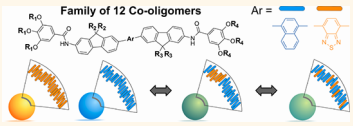

KEYWORDS: dynamics · energy transfer · nanoparticles · self-sorting · supramolecular chemistry

Fluorescent nanoparticles based on π-conjugated polymers and oligomers have attracted much interest lately due to their small size, high fluorescence and photochemical stability, which make them appealing as bioprobes for sensing and imaging.[1−5] In this class of fluorescent systems, the nature of the side chains, that are attached to the π-conjugated backbone play a pivotal role. π-Conjugated polymers functionalized with hydrophobic aliphatic side chains fold into self-assembled static fluorescent nanoparticles (polymer dots),[6−8] while polymers functionalized with hydrophilic or ionic side chains do not form particles but are molecularly dissolved in water.[9−13] In the first case, rigid, stable particles suitable for imaging are formed, while in the latter case, dynamic polymer chains for sensing applications are present that can adapt to the analyte. π-Conjugated block-co-polymers containing both polar and nonpolar side chains that self-assemble into vesicles have been also reported.[14,15]

For π-conjugated oligomers the situation is similar, as oligomers equipped with only nonpolar alkyl tails form self-assembled nanoparticles,[16−23] while oligomers having hydrophilic side chains are molecularly dissolved in water.[24−29] In addition, π-conjugated oligomers containing both hydrophilic and hydrophobic side chains have been made.[30−36] Because of the amphiphilic nature of these molecules, nanoparticles are formed that, in a few cases, have properties similar to membranes and vesicles.[37−39] For example, vesicle-type nanoparticles could be deformed and also vesicle fusion[40] has been found. In the case of multicomponent particles, clustering,[40,41] and multivalency[42] have both been observed.

For imaging and sensing, full control over the stability, dynamics,[43−45] and supramolecular organization[46−49] of the nanoparticles

* Address correspondence to a.p.h.j.schenning@tue.nl.

Received for review September 25, 2012 and accepted December 14, 2012.

Published online December 20, 2012
10.1021/nn305477u

is highly desirable. For example, for imaging and sensing of cells, the dynamic properties within these self-assembled particles could mimic the lateral diffusion of lipids within membranes,[50] thereby enhancing their binding to cells due to the multivalency.[51] However, self-assembled systems generally display equilibrium between monomer and supramolecular architectures,[52] and monomers in solution are usually undesirable for sensing and imaging applications. To date, the stability and dynamic behavior of the self-assembled aqueous structures have been rarely investigated, while it is clear that the side chains of the π-conjugated oligomers play a critical role in these properties.

Recently, we have reported the formation of nanoparticles composed of fluorene co-oligomers forming highly fluorescent nanoparticles.[41] We tuned the emission wavelength of these multicomponent nanoparticles by mixing naphthalene containing donor moieties and benzothiadiazole containing acceptor moieties molecules in one particle and achieved energy transfer. We also showed that the morphology of nanoparticles has an impact on the energy transfer efficiencies. Under the fluorescence microscope, the individual particles were stable showing no exchange of molecules between particles. Furthermore, the nanoparticles could be functionalized with different bioligands at the extremities of inert ethylene glycol side chains, which could be utilized for imaging and sensing.[42]

We have now systematically changed the nature of the side chains of fluorene co-oligomers and investigated its influence on the stability, dynamics, fluorescence, and self-sorting properties of the aqueous self-assembled mono- and bicomponent nanoparticles. We have designed twelve nonionic fluorene derivatives in which we have systematically altered the ratio of hydrophilic ethylene glycol and hydrophobic alkyl side chains (Scheme 1). Naphthalene- and benzothiadiazole-fluorene co-oligomers were chosen to study the above-mentioned properties by energy transfer. Our results show that we can control stability, dynamics, and self-sorting properties by simply changing the nature of the side chains of the π-conjugated oligomers (Scheme 2).

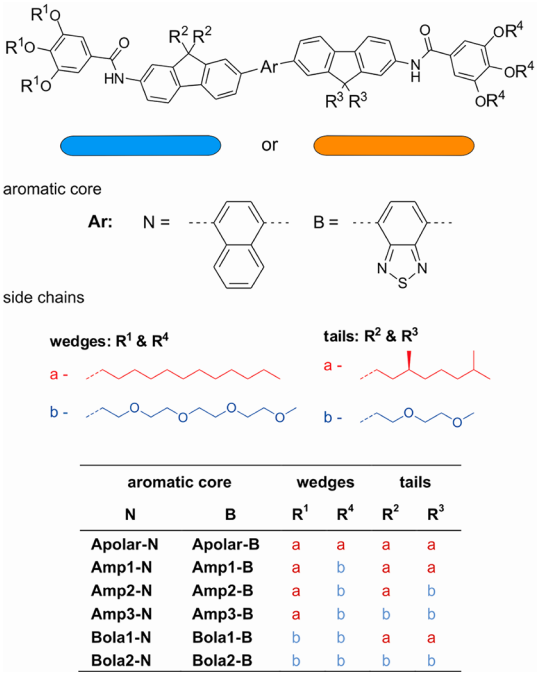

aromatic core		wedges		tails	
N	B	R^1	R^4	R^2	R^3
Apolar-N	Apolar-B	a	a	a	a
Amp1-N	Amp1-B	a	b	a	a
Amp2-N	Amp2-B	a	b	a	b
Amp3-N	Amp3-B	a	b	b	b
Bola1-N	Bola1-B	b	b	a	a
Bola2-N	Bola2-B	b	b	b	b

Scheme 1. Molecular structures of the 12 nonionic fluorene based co-oligomers used for the formation of fluorescent nanoparticles in water. The bars represent the emission color of the π-conjugated core while the colors of the side chains refer to polarity.

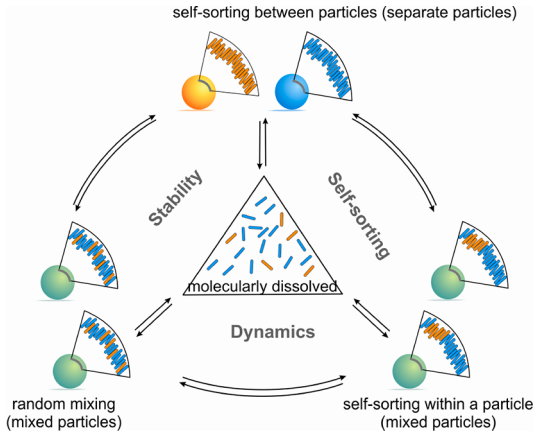

Scheme 2. Different self-assembled states of bi-component nanoparticles, consisting of N and B derivatives (Scheme 1), which have been observed in this study. Equilibriums exist between these states and the two monomers, showing the dynamics between nanoparticles, within a particle, and between particles and monomers.

RESULTS AND DISCUSSION

Molecular Design. We have successfully synthesized two sets (naphthalene (**N**) and benzothiadiazole (**B**) derivatives) of six fluorene co-oligomers in which the number and the substitution pattern of the hydrophobic alkyl and the hydrophilic nonionic side chains on the π-conjugated backbone has been systematically changed (Scheme 1, **Apolar**, **Amp1**, **Amp2**, **Amp3**, **Bola1**, and **Bola2**). For example, the **Apolar** derivatives contain only hydrophobic side chains, while the side chains of **Bola2** derivatives are exclusively hydrophilic ethylene glycols. For the amphiphiles **Amp1**, **Amp2**, and **Amp3** having one apolar and one polar wedge, the tails on the fluorene moieties were gradually altered from hydrophobic to hydrophilic. The wedges of the molecules **Apolar**, **Amp1**−**3**, and **Bola1**,**2** change from two apolar, *via* one apolar and one polar, to two polar wedges in which we name the first one apolar, the second one amphiphilic, and the latter one bolaamphiphilic molecules. The **N** and **B** derivatives act as energy donor and energy acceptor (Scheme 1), respectively, which display only minor changes in the shape and size of the π-conjugated molecule, allowing

TABLE 1. Optical Characteristics, Hydrodynamic Radius and Critical Aggregation Concentration (CAC) of Amphiphilic Derivatives in Water Solution (c = 3 μM)

	wedges[a]		tails[a]		UV−vis absorption[b]	photoluminescence[b]	radius[c]	CAC[d]
	R^1	R^4	R^2	R^3	λ/nm (log(ε)/M^{-1} cm^{-1})	λ_{max}/nm (Φ_{PL}(%))	R_h/nm	M^{-1}
Apolar-N	a	a	a	a	344 (4.82)	422 (60)	54	10^{-10}
Amp1-N	a	b	a	a	338 (4.63)	421 (50)	40	10^{-9}
Amp2-N	a	b	a	b	334 (4.80)	423 (25)	70; 20[e]	10^{-9}
Amp3-N	a	b	b	b	335 (4.78)	429 (30)	78; 15[e]	10^{-8}
Bola1-N	b	b	a	a	331 (4.77)	425 (7)	40	10^{-9}
Bola2-N	b	b	b	b	344 (4.88)	426 (6)	80	10^{-7}
Apolar-B	a	a	a	a	338 (4.74); 431 (4.36)	527 (40)	55	
Amp1-B	a	b	a	a	335 (4.76); 430 (4.35)	528 (85)	39	
Amp2-B	a	b	a	b	332 (4.74); 432 (4.27)	551 (70)	74; 12[e]	
Amp3-B	a	b	b	b	334 (4.71); 429 (4.27)	568 (50)	81; 16[e]	
Bola1-B	b	b	a	a	322 (4.73); 429(4.23)	550 (70)	40	
Bola2-B	b	b	b	b	337 (4.80); 421 (4.40)	578 (15)	81	

[a] See Scheme 1. [b] Data after annealing. For the naphthalene derivatives: excitation wavelength λ_{exc} = 340 nm, reference compound quinine bisulfate in 1 N H_2SO_4; for the benzothiadiazole derivatives: excitation wavelength λ_{exc} = 340 nm, reference compound *N*,*N*′-bis(pentylhexyl) perylene bisimide in dichloromethane. [c,d] Data after annealing. [e] The nanoparticles formed by **Amp2** and **Amp3** in water show two populations.

us to study the dynamic and self-sorting properties in these bicomponent systems by photoinduced energy transfer.[41,53,54] The synthesis of the **Apolar** and **Bola1** derivatives has already been described,[41,53] while the synthesis of the other eight compounds is reported in the Supporting Information (SI). All compounds have been extensively purified and fully characterized (SI).

Formation and Characterization of the Self-Assembled Nanoparticles. Each molecule was injected into water according to the reprecipitation method, annealed at 90 °C for 10 min[55] and analyzed at room temperature to investigate if they all form nanoparticles. In most cases, a decrease of the extinction coefficient and a blue shift of the absorption band were observed (Table 1 and SI, TableS1, FigureS1−FigureS3) when compared with THF, with a maximal shift of 10 nm for **Bola1-N** and **Bola1-B**. It should be noted that the shift of the absorption maximum was different for each component reflecting the role of the side chains on aggregation. A pronounced difference could also be observed for the fluorescence properties of the molecules, with quantum yields ranging from 5 to 55% and from 15 and 85% for naphthalene **N** and benzothiadiazole **B** derivatives, respectively, with the lowest values found for the oligomers that had only polar ethylene glycol tails. The naphthalene compounds **Apolar-N**, **Amp1-N**, **Amp3-N** showed an enhanced quantum yield in water compared to THF, while for all benzothiadiazole derivatives a decrease was observed. The enhancement is probably caused by planarization of the naphthalene−fluorene π-conjugated core leading to lower nonradiative recombination rates while in case of the benzothiadiazole derivatives aggregation induced quenching dominates (*vide infra*).[53,54] The emission maximum peak of the benzothiadiazole nanoparticles in water changed from 529 nm for the most nonpolar oligomer (**Apolar-B**) to the red, 575 nm, for the most polar oligomer (**Bola2-B**). Previous studies revealed that the emission of fluorene−benzothiadiazole copolymers is sensitive to the polarity of its environment, resulting in a red shift and a decrease in emission intensity as the environment becomes more hydrophilic.[56] Most likely, nanoparticles self-assembled from oligomers that have polar ethylene glycol side chains contain more water than nanoparticles self-assembled of oligomers that only contain nonpolar side chains.[57] Circular dichroism (CD) measurements revealed CD effects for the nanoparticles that are formed by the chiral derivatives indicating a helical ordering of the π-conjugated oligomers (SI, Figure S4). Multiangle dynamic light scattering (DLS) showed that all fluorene derivatives formed self-assembled nanoparticles in which, in general, the diameter increased going from the apolar to the polar derivatives (for example **Apolar-N** R_h = 54 nm and **Bola2-N** R_h = 80 nm; Table 1, SI TableS2 and FigureS5). DLS data sets for **Apolar**, **Amp1**, **Bola1**, and **Bola2** derivatives were fitted best with a first order exponential decay, attesting the existence of a single population of nanoparticles. For **Amp2** and **Amp3** nanoparticles in solution, the DLS data shows the presence of two populations reflected by the second order exponential decay and the two resulting diffusive processes.

Some nanoparticles were further characterized by transmission electron microscopy (TEM) and small-angle X-ray scattering (SAXS) revealing a comparable diameter as observed by DLS (Table 1 and SI FigureS6 − FigureS9; an example is given for **Amp1-B** in Figure 1). Small size differences between DLS and TEM, that is, 10 nm for **Amp2-B**, reflect the possible collapse of

the nanoparticles deposited on the carbon substrate for TEM analysis, and thus expansion of the observed object.[58,59] The stability of the nanoparticles, measured by determining the critical aggregation concentration (CAC), decreased upon going to nanoparticles from oligomers containing more polar ethylene glycol side chains (Table 1 and SI, TableS3, FigureS10, and FigureS11).[60]

These results show that all fluorene single component systems formed stable self-assembled fluorescent nanoparticles in water, in which the oligomers were most likely organized both in helical and amorphous domains. The self-assembly of the nanoparticles was strongly influenced by the nature of side chains of the π-conjugated oligomers. The nanoparticles which were self-assembled from oligomers containing polar ethylene glycol side chains were less stable and larger in size. In contrast, the nanoparticles which self-assembled from oligomers containing nonpolar side chains were more stable, smaller and had in general a higher fluorescence quantum yield.

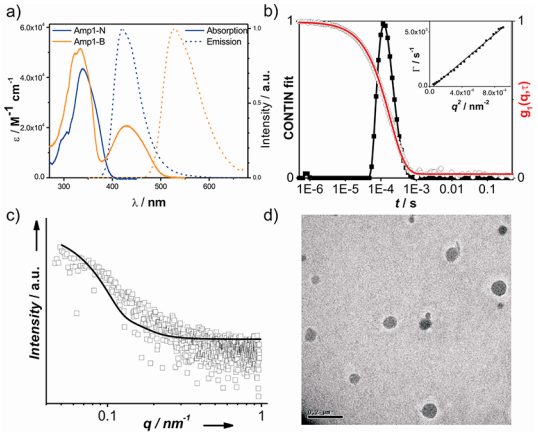

Figure 1. (a) Absorption and emission spectra of self-assembled nanoparticles Amp1-N (blue, λ_{exc} = 340 nm) and Amp1-B (orange, λ_{exc} = 340 nm). (b) Hydrodynamic radius of Amp1-B nanoparticles achieved *via* CONTIN fit of 150° correlation function and single exponential fit of angular data (inset). (c) SAXS profile of Amp1-B nanoparticles. The hollow squares represent the experimental profile. The calculated best fit curve (black line) is achieved assuming particles as spheres of radius 40 nm. (d) Transmission electron microscopy (TEM) image of Amp1-B nanoparticles. The scale bar represents 200 nm. Concentration in all cases, *c* = 3 μM.

Dynamics and Self-Sorting Properties of Self-Assembled Nanoparticles of Two Chromophores with Similar Side Chains. Since all fluorene co-oligomers form particles, the dynamic and self-sorting behavior between the self-assembled aqueous nanoparticles have been investigated by mixing two aqueous solutions of both compounds with similar side chains and subsequent annealing at 90 °C for 10 min (Scheme 3, method A).[54] The photoluminescence (PL) spectra of the **Amp1-B** and **Amp1-N** mixtures in which the ratio between these two molecules has been systematically varied, revealed that the intensity of the donor and acceptor emission is just a sum of the two components (Figure 2a). Furthermore, an isosbestic point was found showing the presence of the only species composed of either **Amp1-B** or **Amp1-N** particles. Plotting the intensity of the donor emission of **Amp1-N** for different **N**-**B** mixtures

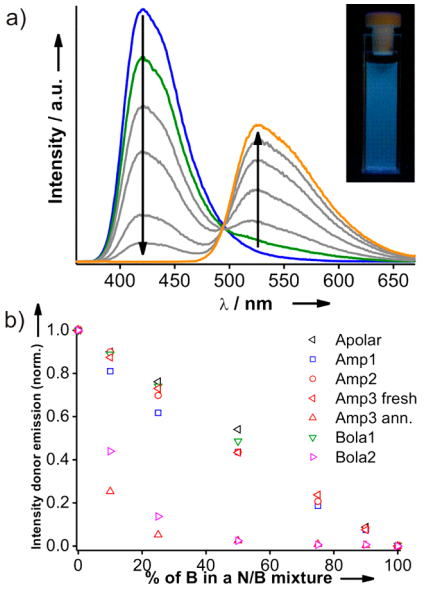

Figure 2. The dynamics and self-sorting of nanoparticles prepared by method A. (a) Emission spectra of separate Amp1-N and Amp1-B nanoparticles in water (100% Amp1-N, blue curve, Amp1-N/Amp1-B: 90:10, green curve, 75:25, 50:50, 25:75, 10:90, gray curves, and 100% Amp1-B, orange curve), after annealing. The inset shows a photograph of the blue fluorescence of a solution of separate nanoparticles (95:5, Amp1-N/Amp1-B). (b) The naphthalene N donor emission intensity (normalized, at λ_{em} = 424 nm) for different N/B mixtures (λ_{exc} = 340 nm, total concentration is always 3 μM).

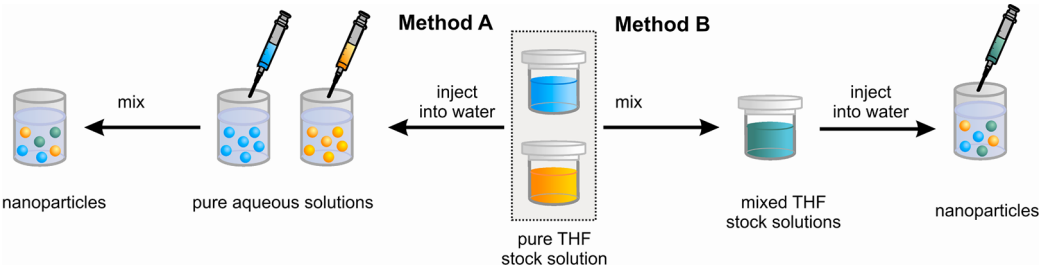

Scheme 3. Schematic illustration of different sample preparation methods to study the dynamics and self-sorting properties of nanoparticles.

TABLE 2. Summary of the Donor Intensity of Nanoparticles in Water Composed of 90% Donor and 10% Acceptor Fluorene-Based Co-Oligomers[a]

		donor intensity[d]	
donor[b]	acceptor[b]	method A[c]	method B[c]
	Similar Wedges and Similar Tails[b]		
Apolar-N	**Apolar-B**	1	0.01
Amp1-N	**Amp1-B**	0.9	0.01
Amp2-N	**Amp2-B**	1	0.04
Amp3-N (fresh)	**Amp3-B**	1	
Amp3-N (ann.)	**Amp3-B**	0.3	0.08
Bola1-N	**Bola1-B**	1	0.1
Bola2-N	**Bola2-B**	0.5	0.5
	Similar Wedges and Distinct Tails[b]		
Amp2-B	**Amp1-B**		0.09
Amp3-B	**Amp1-B**		0.4
	Distinct Wedges and Similar Tails[b]		
Apolar-N	**Bola1-B**		0.5
Amp1-N	**Bola1-B**		0.3
	Distinct Wedges and Distinct Tails[b]		
Bola2-N	**Bola1-B**		0.9

[a] Donor intensities close to 1 reveal separate particles while donor intensities much smaller than 1 reveal mixed particles. [b] See Scheme 1. [c] See Scheme 3. [d] The donor intensity is corrected for the dilution of the donor with the acceptor (total concentration is always 3 μM).

revealed a straight line (Figure 2b and SI, Figure S12) indicating the absence of energy transfer.[54,61] The same behavior was also found for **Apolar**, **Amp2**, and **Bola1** showing no exchange of molecules between the nanoparticles in solution, and disclosed the formation of separate, stable particles, as already found earlier for **Bola1**.[41] In contrast, the **Amp3** system showed no energy transfer for the fresh aqueous solution but energy transfer was observed after annealing. After annealing, the donor emission is halved for the 90:10 (**Amp3-N**/**Amp3-B**) mixture pointing to the formation of mixed nanoparticles (*vide infra*).[1] In the case of **Bola2-B**/**Bola2-N**, energy transfer is already observed before annealing showing ready dynamics between particles at room temperature (Figure 2). Overall, these data reveal that the more apolar systems remain self-sorted after annealing while the polar ones (three out of four side chains are polar, Scheme 1) show dynamics between the self-assembled particles (Table 2). Since the radius of these particles is not changing after annealing this process most likely occurs *via* exchange of monomers (Scheme 2, SI, Figure S13).[40]

To study the dynamics and self-sorting within a single particle, nanoparticles were prepared by mixing **N** and **B** derivatives with similar side chains in THF before injection into water and subsequent annealing (Scheme 3, method B).[54] Energy transfer occurred in all cases (Figure 3 and Table 2). A representative evolution of the fluorescence spectra of mixed nanoparticles of

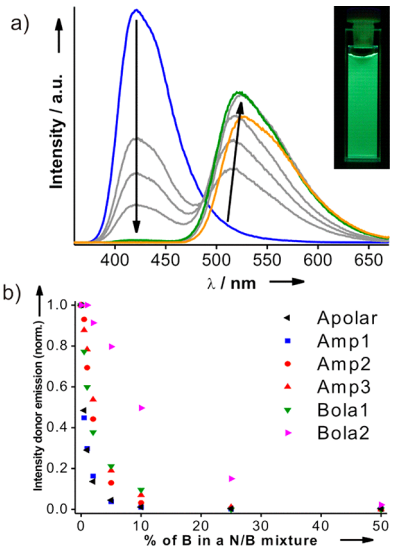

Figure 3. The dynamics and self-sorting of nanoparticles prepared by method B. (a) Emission spectra of mixed Amp1-N/Amp1-B nanoparticles in water as pure Amp1-N (blue curve) followed by 0.5% Amp1-B, 1% Amp1-B, 2% Amp1-B (gray curves), 10% Amp1-B (green curve), 25% Amp1-B (gray curve) mixtures, and pure Amp1-B (orange curve), after annealing. The inset shows a photograph of the yellow greenish fluorescence of a solution of mixed nanoparticles (95: 5, Amp1-N/Amp1-B). (b) The naphthalene donor emission intensity (normalized, at λ = 424 nm) for different N/B mixtures (λ_{exc} = 340 nm, total concentration is always 3 μM).

Amp1 by changing the ratio between donor and acceptor is given in Figure 3a. At already low concentration of acceptor molecules, a pronounced decrease of **Amp1-N** emission (donor) took place, while simultaneously the emission of **Amp1-B** (acceptor) was enhanced. Interestingly, for all systems the energy transfer in the mixed nanoparticles resulted in an enhancement of the fluorescence of the **B** acceptor molecule at low incorporation ratios, more than doubling the emission compared to pure benzothiadiazole nanoparticles (**Bola2-B**; SI, FigureS14). Most likely the enhancement is caused by energy transfer from the naphthalene donors to isolated benzothiadiazole acceptors while for higher percentages of acceptors aggregation (*i.e.*, self-sorting) takes places and therefore quenching occurs.[54] A gradual red shift of about 12 nm in the acceptor emission was observed with increasing concentration of **Amp1-B**, which is caused by nanoparticles with a certain degree of self-sorting.[54] These observations pointed to the formation of mixed particles. Although the **N** and **B** derivatives display only minor changes in size and shape, self-sorting always takes place which might be due to the difference in torsion angle between the fluorene and the central aromatic core **N** (71°) and **B** (40°).[53] Remarkably, for the polar **Bola2** nanoparticles the same decrease in donor emission intensity independent from the preparation method was observed (SI, FigureS15 and FigureS16) revealing that highly dynamic self-assembled particles are formed at room temperature and that the final

outcome of the self-assembly process is determined by thermodynamic parameters (Scheme 2).

Our results show that with method A, there was no exchange of molecules between the particles for the systems **Apolar**, **Amp1**, **Amp2**, and **Bola1** (Scheme 2) while **Bola2** and **Amp3** nanoparticles behaved differently, as they were dynamic and the exchange of molecules between particles took place. This behavior indicates that kinetic self-sorted[48,49] particles were formed for the more apolar systems (**Apolar**, **Amp1**, **Amp2**, and **Bola1**). For the polar **Bola2** nanoparticles the same decrease in donor emission intensity independent from the preparation method was observed. Further, **Amp3** showed exchange of monomers between particles after annealing, revealing for both, **Bola2** and **Amp3**, dynamic nanoparticles (Scheme 2). The fluorescence data obtained by method B suggest the formation of mixed particles with a certain degree of self-sorting.[54] It appears that small differences in the design of amphiphilic molecules can result in tremendous differences in the stability, dynamic and the self-sorting properties of our fluorescent nanoparticles.

Dynamics and Self-Sorting Properties of Self-Assembled Nanoparticles of Two Chromophores with Distinct Side Chains. Finally, the dynamic and self-sorting behavior of the self-assembled aqueous nanoparticles with bicomponent nanoparticles consisting of **N** and **B** derivatives containing different tails and wedges (Scheme 1) has been investigated. Remarkably, separate donor **N** and acceptor **B** nanoparticles in water were formed by injecting a mixed THF solution containing **Bola1-B**/**Bola2-N** (Scheme 3, method B). The fluorescence intensity showed a linear dependence as the donor and acceptor ratio was altered (Figure 4a, SI FigureS17), revealing that no energy transfer occurs. Remarkably, although the nanoparticles are prepared by method B (Scheme 3, mixed THF stock solution) separate nanoparticles were formed. This self-sorting between particles is likely a result of the dynamic behavior of the polar **Bola2-N** at room temperature. Since **Bola1-B** and **Bola2-N** have different tails, the degree of self-sorting is more pronounced in comparison with **N**−**B** systems that have similar side chains, leading to separate **N** and **B** particles. By using the same method, we have also mixed acceptor **Bola1-B** with donor **Amp1-N** and **Apolar-N**, which have similar tails but different wedges. After annealing we observed a nonlinear decrease in intensity of the donor **N** emission for both mixtures in which the decrease was less pronounced than for the **Bola1-B**/**Bola1-N** nanoparticles having the same side chains (Figure 4a, SI FigureS18). Furthermore, we found a red shift in the acceptor **Bola1-B** emission already at low percentages of acceptor (Figure 4b) which is caused by aggregation of **Bola1-B** resulting in a less efficient energy transfer process. Interestingly, the normalized donor **N** emission intensity decreases less for **Bola1-B**/**Apolar-N** compared to **Bola1-B**/**Amp1-N**

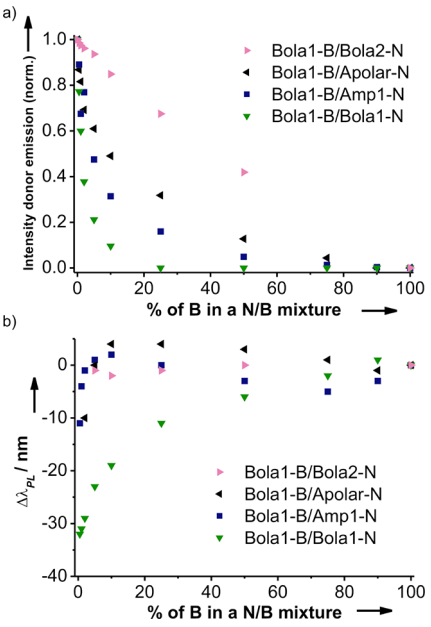

Figure 4. (a) The emission intensity (normalized, at λ = 424 nm) of the donor N and (b) the shift of the emission maximum of acceptor Bola1-B for different N/Bola1-B mixtures and ratios (method B, total concentration is always 3 μM).

(Figure 4a) indicating that the degree of self-sorting of **Bola1-B** is higher in the **Apolar-N** particles in which the differences in polarity of the wedges is totally altered (Scheme 1 and Table 2).

We also mixed the amphiphilic **Amp1-B** into **Amp2-N** and **Amp3-N** compounds, which have the same wedges but different tails on the fluorene moieties. The data also indicate mixed particles in which the degree of self-sorting within the particles can be controlled by the nature of the tails (if the number of different tails is higher, the degree of self-sorting is also higher, Table 2 and SI, FigureS19 and FigureS20). The self-assembly of nanoparticles consisting of π-conjugated oligomers having different side chains caused self-sorting, resulting either in the formation of domains within particles or in the formation of separate nanoparticles depending on the dynamic behavior of the self-assembled π-conjugated oligomers (Scheme 2).

CONCLUSION

We have designed, synthesized, and fully characterized 12 rod−coil fluorescent oligomers that vary in polarity *via* nonpolar, amphiphilic, bola-amphiphilic, to polar, containing either a naphthalene or a benzothiadiazole aromatic core. We have demonstrated that the side chains of π-conjugated oligomers play a key role in the size, stability, fluorescence, dynamic, and self-sorting properties of self-assembled nanoparticles. In general, the fluorescent quantum yield and stability decreased while the dynamics increases when using more polar fluorene derivatives. In the case of bicomponent systems, the exchange of molecules took place between particles only for the most polar fluorene oligomers. Furthermore,

depending on the preparation method, self-sorting particles or more randomly mixed particles could be produced in fluorene derivatives having the same side chains. In the case of oligomers having different side chains, self-sorting took place either between particles or within a single particle in which the degree of self-sorting can be controlled by the number of different side chains. In general the final properties of the nanoparticles depend highly on the preparation protocol in cases where the dynamics between and within the particles is slow.

These novel findings show that by appropriate design of side chains, dynamics and self-sorting behavior of these particles can be tuned making it possible to construct stable, adaptive, highly fluorescent nanoparticles that only show dynamics within particles. Our results not only are important for the development of nanoparticles but also give guidelines for the design of side chains of π-conjugated systems to prepare multicomponent nanomaterials with desired macroscopic properties.

MATERIALS AND METHODS

Synthesis and Characterization. Full details of the synthetic procedure are given in the Supporting Information together with NMR and MALDI TOF mass spectrometry characterization data.

Preparation and Characterization of Nanoparticles. The nanoparticles were prepared by injecting 15 μL of 1 mM THF stock solution into 5 mL of water, which results in a 3 μM nanoparticle solution. Annealing was performed by heating the sample to 90 °C and cooling down to 20 °C. UV−vis, PL, and CD spectra were measured on a Jasco V-650 spectrophometer, a Jasco FP-6500 spectrofluorometer, and a JASCO J-815 CD spectrometer, respectively. The optical density of the samples for fluorescence measurements was below 0.1. Solutions were measured in a liquid cell with a 1 cm path length for UV−vis and 1 mm path length for fluorescence at room temperature. Absorption, emission, and CD spectra for all nanoparticles and compounds in THF can be found in the Supporting Information (Figure S1−S4 and Table S1). Dynamic light scattering experiments (DLS) were performed on an ALVCGS-3 Compact Goniometer, in the angular range of 25 to 151 degrees. The incident beam was produced by a HeNe laser operating at 532 nm. The intensity signal was sent to an ALV5000 digital correlator, using a typical acquisition time of 100 s for each angle. The nanoparticle solutions were prepared *via* the reprecipitation method as described before followed by a filtration *via* a 0.4 μm pore size cellulose filter to remove dust particles. The calculation of the particle size distribution for all nanoparticles was performed using CONTIN fits (SI Figure S5 and Table S2). Visualization by transmission electron microscopy (TEM) was done with a Technai G2 Sphera by FEI, working at a voltage of 200 kV on a CCD chip of 1024 × 1024 pixels. Samples were prepared by dropcasting a 3 μM solution of nanoparticles on a carbon film on a 400 square mesh copper grid for 2 min. TEM images for **Amp1-B**, **Amp2-B**, and **Amp1-B**/**Amp2-B** (9/1) can be found in the Supporting Information (Figure S6). Small-angle X-ray scattering (SAXS) measurements were performed at the Dutch−Belgian BM26B beamline at the ESRF in Grenoble (France). An X-ray photon energy of 10 keV and a sample-to-detector distance (S-to-D) of 7 m were used, which allows a "q- range" of 0.05 $nm^{-1} < q <$ 0.9 nm^{-1}, where q is the momentum transfer vector, related to the angle of incidence (θ) and wavelength (λ) of the X-ray. At the sample position, the collimated beam was focused with a typical cross section of 0.3 × 0.3 mm^2. The SAXS images were recorded using a 2D multiwire gas filled detector. The positions of diffracted peaks from standard Silver Behenate and rat tail collagen samples were used in order to calibrate the experimental q-range. The sample solutions were contained in 1 mm borosilicate capillaries. Standard data reduction procedures, that is, subtraction of the empty capillary contribution, correction for the solvent absorption and dark current *etc.* were applied. SAXS profiles of **Apolar-B**, **Amp1-B**, and **Bola1-B** solutions can be found in the Supporting Information (Figure S7−S9). The critical aggregation concentration (CAC) of the particles was determined by a previous reported method[41] using nanoparticles containing both a naphthalene derivative, as an energy donor, and benzothiadiazole, as an energy acceptor in a ratio of 95: 5. Upon dilution, the energy transfer efficiency was measured. At a certain point an increase of the blue donor emission relative to the yellow acceptor emission was observed, revealing that the nanoparticles started to disassemble, reflecting the CAC (SI Figure S10 and S11).

Preparation and Characterization of Self-Assembled Nanoparticles of Two Chromophores. Energy transfer studies were done using naphthalene derivatives as energy donor and benzothiadiazole as acceptor molecules. Nanoparticles were prepared in two different ways (Scheme 3). In the first method, two THF stock solutions of both compounds were injected into water and the resulting aqueous solutions were mixed (method A) and second, a premixed THF stock solution containing both oligomers was injected into water (method B). The total chromophore concentration remained constant in both cases and the solutions were annealed. The emission spectra from separate nanoparticles of **Apolar**, **Amp1**, **Amp2**, **Amp3**, **Bola1**, and **Bola2** nanoparticles in water (c = 3 μM) after annealing prepared by method A are found in SI Figure S12. The emission spectra of **Apolar**, **Amp1**, **Amp2**, **Amp3**, **Bola1**, and **Bola2** nanoparticles in water (c = 3 μM) for fresh and annealed samples prepared from mixed nanoparticles (method B) are shown in SI Figure S14. The emission spectra of self-assembled nanoparticles of two chromophores with different side chain are represented in SI Figures S17−S20.

Conflict of Interest: The authors declare no competing financial interest.

Supporting Information Available: Synthesis and characterization details for Amp1-N, Amp1-B, Amp2-N, Amp2-B, Amp3-N, Amp3-B, Bola2-N, and Bola2-B; characterization data for Apolar-N, Apolar-B, Amp1-N, Amp1-B, Amp2-N, Amp2-B, Amp3-N, Amp3-B, Bola1-N, Bola1-B, Bola2-N, and Bola2-B nanoparticles (UV−vis, PL, CD, DLS, TEM, SAXS); emission spectra of self-assembled nanoparticles of two chromophores. This material is available free of charge *via* the Internet at http://pubs.acs.org.

Acknowledgment. We thank Ralf Bovee for MALDI-ToF MS measurements. This research has been made possible by The Netherlands Foundation for Scientific Research (NWO) by a VICI grant.

REFERENCES AND NOTES

1. Kaeser, A.; Schenning, A. P. H. J. Fluorescent Nanoparticles Based on Self-Assembled π-Conjugated Systems. *Adv. Mater.* **2010**, *22*, 2985–2997.
2. Herland, A.; Inganäs, O. Conjugated Polymers as Optical Probes for Protein Interactions and Protein Conformations. *Macromol. Rapid Commun.* **2007**, *28*, 1703–1713.
3. Duarte, A.; Pu, K.-Y.; Liu, B.; Bazan, G. C. Recent Advances in Conjugated Polyelectrolytes for Emerging Optoelectronic Applications. *Chem. Mater.* **2011**, *23*, 501–515.
4. Pu, K.; Liu, B. Fluorescent Conjugated Polyelectrolytes for Bioimaging. *Adv. Funct. Mater.* **2011**, *21*, 3408–3423.
5. Zhu, C.; Liu, L.; Yang, Q.; Lv, F.; Wang, S. Water-Soluble Conjugated Polymers for Imaging, Diagnosis, and Therapy. *Chem. Rev.* **2012**, *112*, 4687–4735.
6. Wu, C.; Bull, B.; Szymanski, C.; Christensen, K.; McNeill, J. Multicolor Conjugated Polymer Dots for Biological Fluorescence Imaging. *ACS Nano* **2008**, *2*, 2415–2423.

7. Pecher, J.; Mecking, S. Nanoparticles of Conjugated Polymers. *Chem. Rev.* **2010**, *110*, 6260–6279.
8. Tuncel, D.; Demir, H. V. Conjugated Polymer Nanoparticles. *Nanoscale* **2010**, *2*, 484–494.
9. Swager, T. M. The Molecular Wire Approach to Sensory Signal Amplification. *Acc. Chem. Res.* **1998**, *31*, 201–207.
10. Thomas, S. W.; Joly, G. D.; Swager, T. M. Chemical Sensors Based on Amplifying Fluorescent Conjugated Polymers. *Chem. Rev.* **2007**, *107*, 1339–1386.
11. Feng, X.; Liu, L.; Wang, S.; Zhu, D. Water-Soluble Fluorescent Conjugated Polymers and Their Interactions with Biomacromolecules for Sensitive Biosensors. *Chem. Soc. Rev.* **2010**, *39*, 2411–2419.
12. Achyuthan, K. E.; Bergstedt, T. S.; Chen, L.; Jones, R. M.; Kumaraswamy, S.; Kushon, S. A.; Ley, K. D.; Lu, L.; McBranch, D.; Mukundan, H.; *et al*. Fluorescence Superquenching of Conjugated Polyelectrolytes: Applications for Biosensing and Drug Discovery. *J. Mater. Chem.* **2005**, *15*, 2648–2656.
13. Jiang, H.; Taranekar, P.; Reynolds, J. R.; Schanze, K. S. Conjugated Polyelectrolytes: Synthesis, Photophysics, and Applications. *Angew. Chem., Int. Ed.* **2009**, *48*, 4300–4316.
14. Gutacker, A.; Adamczyk, S.; Helfer, A.; Garner, L. E.; Evans, R. C.; Fonseca, S. M.; Knaapila, M.; Bazan, G. C.; Burrows, H. D.; Scherf, U. All-Conjugated Polyelectrolyte Block Copolymers. *J. Mater. Chem.* **2009**, *20*, 1423–1430.
15. Scherf, U.; Adamczyk, S.; Gutacker, A.; Koenen, N. All Conjugated Rod−Rod Block Copolymers-Generation and Self-Assembly Properties. *Macromol. Rapid Commun.* **2009**, *30*, 1059–1065.
16. Park, D. H.; Jo, S. G.; Hong, Y. K.; Cui, C.; Lee, H.; Ahn, D. J.; Kim, J.; Joo, J. Highly Bright and Sharp Light Emission of a Single Nanoparticle of Crystalline Rubrene. *J. Mater. Chem.* **2011**, *21*, 8002–8007.
17. Vijayakumar, C.; Sugiyasu, K.; Takeuchi, M. Oligofluorene-Based Electrophoretic Nanoparticles in Aqueous Medium as a Donor Scaffold for Fluorescence Resonance Energy Transfer and White-Light Emission. *Chem. Sci.* **2011**, *2*, 291–294.
18. Adhikari, R. M.; Shah, B. K.; Palayangoda, S. S.; Neckers, D. C. Solvent Dependant Optical Switching in Carbazole-Based Fluorescent Nanoparticles. *Langmuir* **2009**, *25*, 2402–2406.
19. An, B.; Kwon, S.; Park, S. Y. Photopatterned Arrays of Fluorescent Organic Nanoparticles. *Angew. Chem., Int. Ed.* **2007**, *46*, 1978–1982.
20. Tachikawa, T.; Chung, H.-R.; Masuhara, A.; Kasai, H.; Oikawa, H.; Nakanishi, H.; Fujitsuka, M.; Majima, T. *In Situ* and *Ex Situ* Observations of the Growth Dynamics of Single Perylene Nanocrystals in Water. *J. Am. Chem. Soc.* **2006**, *128*, 15944–15945.
21. Kim, H.-J.; Lee, J.; Kim, T.-H.; Lee, T. S.; Kim, J. Highly Emissive Self-Assembled Organic Nanoparticles Having Dual Color Capacity for Targeted Immunofluorescence Labeling. *Adv. Mater.* **2008**, *20*, 1117–1121.
22. Zhang, H.; Wang, D.; Butler, R.; Campbell, N. L.; Long, J.; Tan, B.; Duncalf, D. J.; Foster, A. J.; Hopkinson, A.; Taylor, D.; *et al.* Formation and Enhanced Biocidal Activity of Water-Dispersable Organic Nanoparticles. *Nat. Nano* **2008**, *3*, 506–511.
23. Balan, B.; Vijayakumar, C.; Ogi, S.; Takeuchi, M. Oligofluorene-Based Nanoparticles in Aqueous Medium: Hydrogen Bond Assisted Modulation of Functional Properties and Color Tunable FRET Emission. *J. Mater. Chem.* **2012**, *22*, 11224–11234.
24. Xing, C.; Liu, L.; Shi, Z.; Li, Y.; Wang, S. Synthesis of Zwitterionic Water-Soluble Oligofluorenes with Good Light-Harvesting Ability. *Adv. Funct. Mater.* **2010**, *20*, 2175–2180.
25. Liu, B.; Gaylord, B. S.; Wang, S.; Bazan, G. C. Effect of Chromophore-Charge Distance on the Energy Transfer Properties of Water-Soluble Conjugated Oligomers. *J. Am. Chem. Soc.* **2003**, *125*, 6705–6714.
26. Wang, S.; Liu, B.; Gaylord, B. S.; Bazan, G. C. Size-Specific Interactions Between Single- and Double-Stranded Oligonucleotides and Cationic Water-Soluble Oligofluorenes. *Adv. Funct. Mater.* **2003**, *13*, 463–467.
27. Tang, Y.; Zhou, Z.; Ogawa, K.; Lopez, G. P.; Schanze, K. S.; Whitten, D. G. Synthesis, Self-Assembly, and Photophysical Behavior of Oligo Phenylene Ethynylenes: From Molecular to Supramolecular Properties. *Langmuir* **2008**, *25*, 21–25.
28. Ortony, J. H.; Chatterjee, T.; Garner, L. E.; Chworos, A.; Mikhailovsky, A.; Kramer, E. J.; Bazan, G. C. Self-Assembly of an Optically Active Conjugated Oligoelectrolyte. *J. Am. Chem. Soc.* **2011**, *133*, 8380–8387.
29. Janssen, P. G. A.; Jonkheijm, P.; Thordarson, P.; Gielen, J. C.; Christianen, P. C. M.; Dongen, J. L. J.; van; Meijer, E. W.; Schenning, A. P. H. J. Tuning the Self-Assembly of a Ditopic Crown Ether Functionalized Oligo(*p*-phenylenevinylene). *J. Mater. Chem.* **2007**, *17*, 2654–2660.
30. Zhu, L.; Yang, C.; Qin, J. An Aggregation-Induced Blue Shift of Emission and the Self-Assembly of Nanoparticles from a Novel Amphiphilic Oligofluorene. *Chem. Commun.* **2008**, *47*, 6303–6305.
31. Koizumi, Y.; Seki, S.; Tsukuda, S.; Sakamoto, S.; Tagawa, S. Self-Condensed Nanoparticles of Oligofluorenes with Water-Soluble Side Chains. *J. Am. Chem. Soc.* **2006**, *128*, 9036–9037.
32. Rijn, P.; van; Janeliunas, D.; Brizard, A. M. A.; Stuart, M. C. A.; Eelkema, R.; van Esch, J. H. Introduction of Curvature in Amphipathic Oligothiophenes for Defined Aggregate Formation. *Chem.—Eur. J.* **2010**, *16*, 13417–13428.
33. Kumar, M.; George, S. J. Green Fluorescent Organic Nanoparticles by Self-assembly Induced Enhanced Emission of a Naphthalene Diimide Bolaamphiphile. *Nanoscale* **2011**, *3*, 2130–2133.
34. Kim, H.-J.; Kim, T.; Lee, M. Responsive Nanostructures from Aqueous Assembly of Rigid−Flexible Block Molecules. *Acc. Chem. Res.* **2010**, *44*, 72–82.
35. Ryu, J.-H.; Hong, D.-J.; Lee, M. Aqueous Self-Assembly of Aromatic Rod Building Blocks. *Chem. Commun.* **2008**, 1043–1054.
36. Lim, Y.; Moon, K.-S.; Lee, M. Rod−Coil Block Molecules: Their Aqueous Self-Assembly and Biomaterials Applications. *J. Mater. Chem.* **2008**, *18*, 2909–2918.
37. Zhang, X.; Chen, Z.; Würthner, F. Morphology Control of Fluorescent Nanoaggregates by Co-Self-Assembly of Wedge- and Dumbbell-Shaped Amphiphilic Perylene Bisimides. *J. Am. Chem. Soc.* **2007**, *129*, 4886–4887.
38. Zhang, X.; Rehm, S.; Safont-Sempere, M. M.; Würthner, F. Vesicular Perylene Dye Nanocapsules as Supramolecular Fluorescent pH Sensor Systems. *Nat. Chem.* **2009**, *1*, 623–629.
39. Seo, S. H.; Chang, J. Y.; Tew, G. N. Self-Assembled Vesicles from an Amphiphilic ortho-Phenylene Ethynylene Macrocycle. *Angew. Chem., Int. Ed.* **2006**, *45*, 7526–7530.
40. Hoeben, F. J. M.; Shklyarevskiy, I. O.; Pouderoijen, M. J.; Engelkamp, H.; Schenning, A. P. H. J.; Christianen, P. C. M.; Maan, J. C.; Meijer, E. W. Direct Visualization of Efficient Energy Transfer in Single Oligo(p-phenylene Vinylene) Vesicles. *Angew. Chem., Int. Ed.* **2006**, *45*, 1232–1236.
41. Abbel, R.; Weegen, R. van der; Meijer, E. W.; Schenning, A. P. H. J. Multicolour Self-Assembled Particles of Fluorene-Based Bolaamphiphiles. *Chem. Commun.* **2009**, *13*, 1697–1699.
42. Petkau, K.; Kaeser, A.; Fischer, I.; Brunsveld, L.; Schenning, A. P. H. J. Pre- and Postfunctionalized Self-Assembled π-Conjugated Fluorescent Organic Nanoparticles for Dual Targeting. *J. Am. Chem. Soc.* **2011**, *133*, 17063–17071.
43. Rybtchinski, B. Adaptive Supramolecular Nanomaterials Based on Strong Noncovalent Interactions. *ACS Nano* **2011**, *5*, 6791–6818.
44. Krieg, E.; Rybtchinski, B. Noncovalent Water-Based Materials: Robust yet Adaptive. *Chem.—Eur. J.* **2011**, *17*, 9016–9026.
45. Percec, V.; Wilson, D. A.; Leowanawat, P.; Wilson, C. J.; Hughes, A. D.; Kaucher, M. S.; Hammer, D. A.; Levine, D. H.; Kim, A. J.; Bates, F. S.; *et al*. Self-Assembly of Janus Dendrimers into Uniform Dendrimersomes and Other Complex Architectures. *Science* **2010**, *328*, 1009–1014.
46. Das, A.; Molla, M. R.; Banerjee, A.; Paul, A.; Ghosh, S. Hydrogen-Bonding Directed Assembly and Gelation of Donor−Acceptor Chromophores: Supramolecular Reorganization from a Charge-Transfer State to a Self-Sorted State. *Chem.—Eur. J.* **2011**, *17*, 6061–6066.

47. Wang, Y.; Xu, H.; Zhang, X. Tuning the Amphiphilicity of Building Blocks: Controlled Self-Assembly and Disassembly for Functional Supramolecular Materials. *Adv. Mater.* **2009**, *21*, 2849–2864.
48. Osowska, K.; Miljanić, O. Kinetic and Thermodynamic Self-Sorting in Synthetic Systems. *Synlett* **2011**, *2011*, 1643–1648.
49. Safont-Sempere, M. M.; Fernández, G.; Würthner, F. Self-Sorting Phenomena in Complex Supramolecular Systems. *Chem. Rev.* **2011**, *111*, 5784–5814.
50. Lingwood, D.; Simons, K. Lipid Rafts as a Membrane-Organizing Principle. *Science* **2010**, *327*, 46–50.
51. Mammen, M.; Choi, S.-K.; Whitesides, G. M. Polyvalent Interactions in Biological Systems: Implications for Design and Use of Multivalent Ligands and Inhibitors. *Angew. Chem., Int. Ed.* **1998**, *37*, 2754–2794.
52. Greef, T. F. A. De; Smulders, M. M. J.; Wolffs, M.; Schenning, A. P. H. J.; Sijbesma, R. P.; Meijer, E. W. Supramolecular Polymerization. *Chem. Rev.* **2009**, *109*, 5687–5754.
53. Abbel, R.; der Weegen, R. van; Pisula, W.; Surin, M.; Leclère, P.; Lazzaroni, R.; Meijer, E. W.; Schenning, A. P. H. J. Multicolour Self-Assembled Fluorene Co-Oligomers: From Molecules to the Solid State *via* White-Light-Emitting Organogels. *Chem.—Eur. J.* **2009**, *15*, 9737–9746.
54. Stevens, A. L.; Kaeser, A.; Schenning, A. P. H. J.; Herz, L. M. Morphology-Dependent Energy Transfer Dynamics in Fluorene-Based Amphiphile Nanoparticles. *ACS Nano* **2012**, *6*, 4777–4787.
55. The influence of the annealing time was not investigated in detail.
56. Pu, K.-Y.; Cai, L.; Liu, B. Design and Synthesis of Charge-Transfer-Based Conjugated Polyelectrolytes as Multicolor Light-Up Probes. *Macromolecules* **2009**, *42*, 5933–5940.
57. Probably, the difference in stability and quantum yield is due to a different amount of water in the nanoparticles. The detailed analysis of the role of the side chains on the fluorescence quantum yield and the diameter of the single component nanoparticles will be published elsewhere.
58. Friedrich, H.; Frederik, P. M.; With, G. de; Sommerdijk, N. A. J. M. Imaging of Self-Assembled Structures: Interpretation of TEM and Cryo-TEM Images. *Angew. Chem., Int. Ed.* **2010**, *49*, 7850–7858.
59. Orlova, E. V.; Saibil, H. R. Structural Analysis of Macromolecular Assemblies by Electron Microscopy. *Chem. Rev.* **2011**, *111*, 7710–7748.
60. For the determination of the CAC the samples were not annealed to avoid self-sorting of the self-assembled system which hampers the determination of the CAC.
61. The corresponding curves for the acceptor emission peak have a contribution from the donor and energy transfer. Therefore, the donor emission was chosen as a measure for the degree of self-sorting.